Ceres Extinction due to Quantum Gravity Effect

Huaiyang Cui
Department of Physics, Beihang University, Beijing, 102206, China
Email: hycui@buaa.edu.cn
(June 13, 2023, submitted to viXra)

Abstract: In recent years, de Broglie matter wave has been generalized to the solar system on planetary scale, this approach provides a new method for testing quantum gravity effects. This paper shows that the generalized matter wave can quantize the orbits of eight planets correctly, but the orbit of Ceres (dwarf) is forbidden in terms of the quantum gravity theory. This forbidden orbit successfully explains why Ceres is almost extinct in the solar system.

1. Introduction

This year is 100th anniversary of the initiative of de Broglie matter wave [1][2][3]. Traditional quantum theory cannot properly deal with some gravity problems [3][4][5]. In recent years, generalized relativistic matter wave has been proposed and applied to the solar system to explain quantum gravity effects, this approach provides a new method for testing quantum gravity effects. Consider a particle, its relativistic matter wave is given by the path integral

$$\psi = \exp(\frac{i\beta}{c^3}\int_0^x (u_1 dx_1 + u_2 dx_2 + u_3 dx_3 + u_4 dx_4)) \quad . \tag{1}$$

where u is the 4-velocity of the particle, β is the ultimate acceleration [6] determined by experiments. This paper show that the generalized matter wave can quantize the orbits of eight planets correctly, but the orbit of Ceres (dwarf) is forbidden in terms of the quantum gravity theory.

2. Extracting relativistic matter wave from the solar system

In the orbital model as shown in Fig.1(a), the orbital circumference is n multiple of the wavelength of the relativistic matter wave, according to Eq. (1), consider a point on the equatorial plane, we have

$$\left.\begin{array}{c} \frac{\beta}{c^3}\oint_L v_l dl = 2\pi n \\ v_l = \sqrt{\frac{GM}{r}} \end{array}\right\} \Rightarrow \quad \sqrt{r} = \frac{c^3}{\beta\sqrt{GM}} n; \quad n = 0,1,2,\ldots \quad . \tag{2}$$

This orbital quantization rule only achieves a half success in the solar system, as shown in Fig.1(b), the Sun, Mercury, Venus, Earth and Mars satisfy the quantization equation; while other outer planets fail. But, since we only study quantum gravity effects among the Sun, Mercury, Venus, Earth and Mars, so this orbital quantization

rule is good enough as a foundational quantum theory. In Fig.1(b), the blue straight line expresses a linear regression relation among the quantized orbits, so it gives β=2.956391e+10 (m/s^2) by fitting the line. The quantum numbers n=3,4,5,... were assigned to the solar planets, the sun was assigned a quantum number n=0 because the sun is in the **central state**.

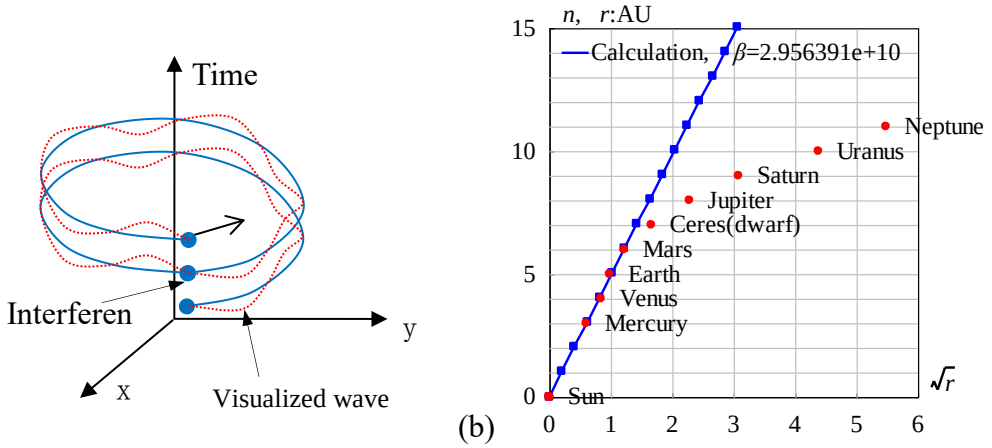

Fig.1 (a)The head of the relativistic matter wave may overlap with its tail. (b) The inner planets are quantized.

The relativistic matter wave can be applied to determine the solar density and radius. In a central state, if the coherent length of the relativistic matter wave is long enough, its head may overlap with its tail when the particle moves in a closed orbit, as shown in Fig.1(a). Consider a point on the equatorial plane, the overlapped wave is given by

$$\psi = \psi(r)T(t)$$

$$\psi(r) = 1 + e^{i\delta} + e^{i2\delta} + \ldots + e^{i(N-1)\delta} = \frac{1-\exp(iN\delta)}{1-\exp(i\delta)} \quad . \tag{3}$$

$$\delta(r) = \frac{\beta}{c^3}\oint_L (v_l)dl = \frac{2\pi\beta\omega r^2}{c^3}$$

where N is the overlapping number which is determined by the coherent length of the relativistic matter wave, δ is the phase difference after one orbital motion, ω is the angular speed of the solar self-rotation. The above equation is a multi-slit interference formula in optics, for a larger N it is called as the Fabry-Perot interference formula.

The relativistic matter wave function ψ needs a further explanation. In quantum mechanics, $|\psi|^2$ equals to the probability of finding an electron due to Max Burn's explanation; in astrophysics, $|\psi|^2$ equals to the probability of finding a nucleon (proton or neutron) *averagely on an astronomic scale*, we have

$$|\psi|^2 \propto \text{nucleon-density} \propto \rho \quad . \tag{4}$$

It follows from the multi-slit interference formula that the overlapping number N is estimated by

$$N^2 = \frac{|\psi(0)_{multi-wavelet}|^2}{|\psi(0)_{one-wavelet}|^2} = \frac{\rho_{core}}{\rho_{surface\_gas}} \quad . \tag{5}$$

The solar core has a mean density of 1408 (kg/m^3), the surface of the sun is comprised of convective zone with a mean density of 2e-3 (kg/m^3) [7]. In this paper, the sun's radius is chosen at a location where density is 4e-3 (kg/m^3), thus the solar overlapping number N is calculated to be N=593. Since the mass density has spherical symmetry, then the ψ has the spherical symmetry.

Sun's angular speed at its equator is known as $\omega=2\pi/(25.05\text{x}24\text{x}3600)$ (s^{-1}). Its mass 1.9891e+30 (kg), well-known radius 6.95e+8 (m), mean density 1408 (kg/m^3), the constant β=2.956391e+10 (m/s^2). According to the N=593, the matter distribution of the $|\psi|^2$ is calculated in Fig.2(a), it agrees well with the general description of star's interior [8]. The radius of the sun is determined as r=7e+8 (m) with a relative error of 0.72% in Fig.2, which indicates that the sun radius strongly depends on the sun's self-rotation.

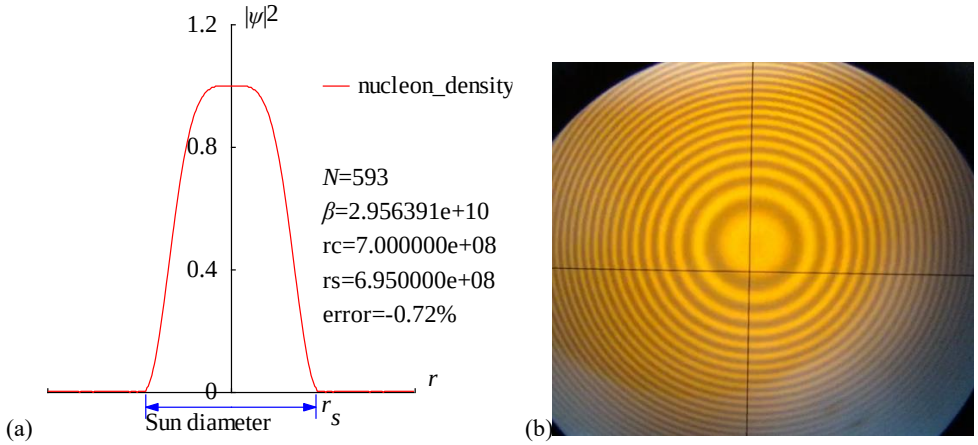

Fig.2 (a)The nucleon distribution $|\psi|^2$ in the Sun is calculated in the radius direction. (b) As contrast, sodium Fabry-Perot interference (δ=const.).

```
<Clet2020 Script>//C source code [9]
int i,j,k,m,n,N,nP[10];
double beta,H,B,M,r,r_unit,x,y,z,delta,D[1000],S[1000], a,b,rs,rc,omega,atm_height; char str[100];
main(){k=150;rs=6.95e8;rc=0;x=25.05;omega=2*PI/(x*24*3600);n=0; a=1408/0.004; N=sqrt(a);
beta=2.956391e10;H=SPEEDC*SPEEDC*SPEEDC/beta;M=1.9891E30; atm_height=2e6; r_unit=1E7;
for(i=-k;i<k;i+=1) {r=abs(i)*r_unit;
if(r<rs+atm_height) delta=2*PI*omega*r*r/H; else delta=2*PI*sqrt(GRAVITYC*M*r)/H;//around the star
x=1;y=0; for(j=1;j<N;j+=1) { z=delta*j; x+=cos(z);y+=sin(z);} z=x*x+y*y; z=z/(N*N);
S[n]=i;S[n+1]=z; if(i>0 && rc==0 && z<0.0001) rc=r; n+=2;}
SetAxis(X_AXIS,-k,0,k,"#ifr; ; ; ;");SetAxis(Y_AXIS,0,0,1.2,"#if|ψ|#su2#t;0;0.4;0.8;1.2;");
DrawFrame(FRAME_SCALE,1,0xafffaf); z=100*(rs-rc)/rs;
SetPen(1,0xff0000);Polyline(k+k,S,k/2,1," nucleon_density"); SetPen(1,0x0000ff);
r=rs/r_unit;y=-0.05;D[0]=-r;D[1]=y;D[2]=r;D[3]=y; Draw("ARROW,3,2,XY,10,100,10,10,",D);
Format(str,"#ifN#t=%d#n#ifβ#t=%e#nrc=%e#nrs=%e#nerror=%.2f%",N,beta,rc,rs,z);
TextHang(k/2,0.7,0,str);TextHang(r+5,y/2,0,"#ifr#sds#t");TextHang(-r,y+y,0,"Sun diameter");
}#v07=?>A
```

3. Improvement

Coherent length and coherent width are two the most important properties of relativistic matter wave. In electronic quantum mechanics, ones almost completely ignore the coherent width and its consequences. Fig.3 illustrates the coherent width concept about the Orbit3 in astrophysics, actually the coherent width covers a range that the gravity can reach until the gravitational influence can be neglected.

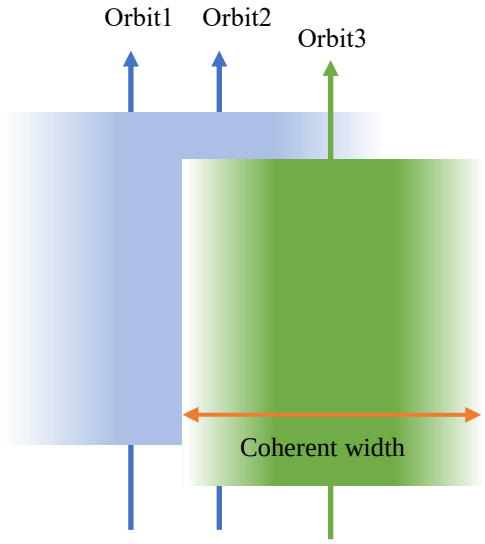

Fig.3 Illustration of the coherent width concept about the orbit3, actually the coherent width covers a range that its gravity can reach until the gravity influence can be neglected.

Because of the coherence width, a planet in the solar system would experience the interaction between its orbit and other seven other orbits, this combined interaction would cause a phase shift for its relativistic matter wave as follows

$$\psi(\varphi) = \exp(\frac{i\beta}{c^3}\int_0^{\varphi}(v+\Delta R)rd\varphi') \quad . \tag{6}$$

Like air friction of rocket or car, suppose that the phase shift term ΔR is proportional to the planet speed, we have

$$\psi(\varphi) = \exp(\frac{i\beta}{c^3}\int_0^{\varphi}(v+\gamma v)rd\varphi') \quad . \tag{7}$$

where the γ is the phase shift coefficient, apparently, $\gamma<0$ would cause a red shift phenomenon for the wavelength of the relativistic matter.

The planet considered moves around the sun on a circular orbit L, imposed the circular quantization condition by its relativistic matter wave as

$$\frac{\beta}{c^3}\oint_L(v+\gamma v)dl = 2\pi n; \quad n = 0,1,2,\ldots \quad . \tag{8}$$

Substituting its speed, we have

$$2\pi n = \frac{\beta}{c^3}\int_0^{2\pi}\sqrt{\frac{GM}{r}}(1+\gamma)rd\varphi' = \frac{2\pi\beta}{c^3}\sqrt{GMr}(1+\gamma) \quad . \tag{9}$$

The first term in the right-hand side of the above equation represents the universal gravitational effect, the second term represents the mean contribution due to coherent width concept which is assumed by

$$\Delta R = \gamma v = Ae^{-r_R/r}\sqrt{\frac{GM}{r}} \quad . \tag{10}$$

where r_R is the location of the peak of ΔR, A is a constant, as illustrated in Fig.4(a).

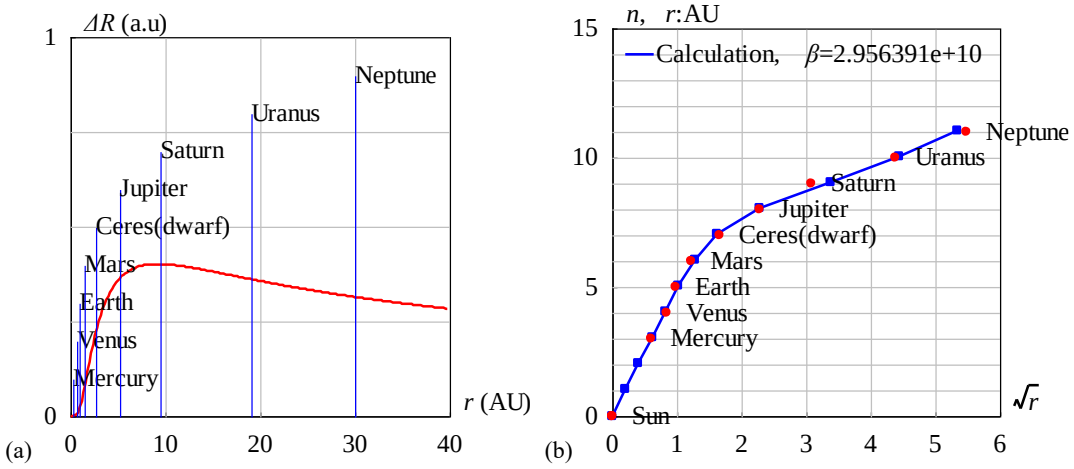

. Fig.4 (a) The interference of relativistic matter waves in their width directions provides the phase retardation.

(b) The outer planets are quantized correctly by the relativistic matter waves.

```
<Clet2020 Script>//[9] sun
char str[200];int i,j,k,N,nP[10]; double x,y,z,D[400],S[400];
double orbit[20]={0,0.3870,0.7233,1,1.5236,2.78,5.2033,9.5370,19.1912,30.0689,};
char Stars[100]={"Sun;Mercury;Venus;Earth;Mars;Ceres(dwarf);Jupiter;Saturn;Uranus;Neptune;"};
main(){ N=200;k=40; D[0]=;D[1]=0;
SetAxis(X_AXIS,0,0,k,"#ifr#t (AU);0;10;20;30;40;");
SetAxis(Y_AXIS,0,0,1,"#ifΔR#t (a.u);0;1;");
DrawFrame(0x0144,1,0xafffaf);
for(i=;i<200;i+=1) {x=k*i/N; y=sqrt(x); z=-4.6/x; y=2*exp(z)/y;
D[i+i]=x;D[i+i+1]=y;}
SetPen(2,0xff0000);Polyline(i,D); nP[0]=TAKE; N=10;SetPen(1,0xff);
for(i=1;i<N;i+=1) { nP[1]=i;TextJob(nP,Stars,str);D[0]=orbit[i];D[1]=0;D[2]=orbit[i];D[3]=0.1*i;
Draw("LINE,0,2,XY,0",D);
TextHang(D[0],D[3],0,str);}
}#v07=?>A
```

We take r_R=4.6AU, A=-0.57, then the outer planets are quantized correctly by the relativistic matter waves, as shown in Fig.4(b).

```
<Clet2020 Script>//[9] sun
char str[200];int i,j,k,N,N1,nP[10],Figure; double x,y,z,r,r1,M,r_unit,H,beta,pD[10],D[400],S[400];
double orbit[20]={0,0.3870,0.7233,1,1.5236,2.78,5.2033,9.5370,19.1912,30.0689,},a,b,c,r_f,A,R;
double e[20]={0,0.2056,0.0067,0.0167,0.0934,0.0483,0.0541,0.0471,0.0085,};
int qn[20]={0,3,4,5,6,7,8,9,10,11,12,13,14,15};
char Stars[100]={"Sun;Mercury;Venus;Earth;Mars;Ceres(dwarf);Jupiter;Saturn;Uranus;Neptune;"};
main(){ Figure=2; N=10;N1=5;M=1.9891E30;r_unit=1.496E11;
for(i=0;i<N;i+=1) {x=orbit[i];y=e[i]; z=x*(1+sqrt(1-y*y))/2; D[i+i]=sqrt(z); D[i+i+1]=qn[i]; }
nP[0]=REGRESSION; nP[1]=N1; DataJob(nP,D,pD); a=pD[0]; b=pD[1]; H=sqrt(GRAVITYC*M*r_unit)/b;
beta=SPEEDC*SPEEDC*SPEEDC/H; c=beta*sqrt(GRAVITYC*M*r_unit)/SPEEDC*SPEEDC*SPEEDC;
S[0]=0;S[1]=0; N=200;r_f=-4.6; A=-0.68;
SetAxis(X_AXIS,0,0,6,"#if#rsr#t;0;1;2;3;4;5;6;"); SetAxis(Y_AXIS,0,0,15,"#ifn#t;0;5;10;15;");
DrawFrame(0x0163,1,0xafffaf); SetPen(2,0xafffaf); k=1; N1=1000;
for(i=0;i<N1;i+=1) { r=35*i/N1; r1=sqrt(r);
if(Figure==1) y=a+b*r1; else y=b*r1*(1+A*exp(r_f/r));
if(y>k) {S[k+k]=r1; S[k+k+1]=y; k+=1; } if(y>15) break;}
Format(str,"Calculation");//TextAt(100,20,"#ifβ#t=%e",beta);
SetPen(2,0x0000ff); Polyline(k,S,0.5,13,str);Plot("CARDFILL,0,@k,XY,3,3,",S);
SetPen(2,0xff0000); Plot("OVALFILL,0,@k,XY,3,3,",D); nP[0]=TAKE;
for(i=0;i<N;i+=1) { nP[1]=i;TextJob(nP,Stars,str); TextHang(D[i+i]+0.4,D[i+i+1],0,str);}
}#v07=?>A
```

4. Band structure in the solar system: extinct Ceres

In electronic quantum mechanics, many-electron system such as in crystals will form a band structure for their energy levels, the same thing will happen in planetary system. For convenience, we define circular wave number k and mean shift F by

$$k \equiv \frac{\beta}{c^3}\sqrt{GMr}; \quad F \equiv \gamma\frac{\beta}{c^3}\sqrt{GMr} = \gamma k \quad . \tag{11}$$

The circular orbital quantization equation becomes

$$2\pi n = 2\pi k + 2\pi F \quad . \tag{12}$$

In order to scrutinize its band structure, suppose that each band contains N orbits, we calculate it by

$$\begin{aligned} \cos(\frac{2\pi n}{N}) &= \cos(\frac{2\pi k}{N} + \frac{2\pi F}{N}) \\ &= \cos(\frac{2\pi k}{N})\cos(\frac{2\pi F}{N}) + \sin(\frac{2\pi k}{N})\sin(\frac{2\pi F}{N}) \end{aligned} \quad . \tag{13}$$

Because the shift F is regarded as a smaller quantity, we approximately obtain

$$\cos(\frac{2\pi n}{N}) \simeq \cos(\frac{2\pi k}{N}) + \frac{2\pi F}{N}\sin(\frac{2\pi k}{N}) \quad . \tag{14}$$

This is in the form of the energy band formula in electronics. As shown in Fig.5(a), where suppose that the farther the orbital radius, the weaker the shift F. This equation determines the possible values of k, and hence the allowed orbits whose $2\pi k/N$ are confined within $|\cos(2\pi n/N)|<1$ while the curve $f(k)=\cos(2\pi k/N)+(2\pi F/N)\sin(2\pi F/N)$ may stray outside the range (-1,+1). On the $2\pi k/N$ scale, the forbidden orbits form gaps separated by bands of allowed orbits, as shown in Fig.5(b).

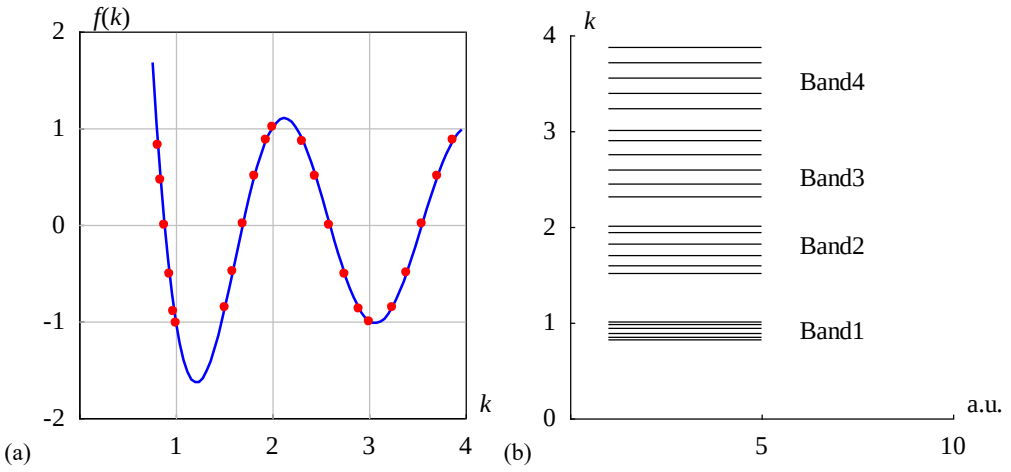

Fig.5 (a) the allowed orbits whose k are confined within $|\cos(2\pi n/N)|<1$. (b) The band structure of orbits on the k scale.

```
<Clet2020 Script>//[9] sun
int i,j,k,n,N,N1,f,Figure; double x,y,z,z1,a,b,c,d,D[400],S[400];
main(){ SetAxis(X_AXIS,0,0,4,"#ifk#t; ;1;2;3;4;"); SetAxis(Y_AXIS,-2,-2,2,"#iff(k)#t;-2;-1;0;1;2;");
DrawFrame(0x0144,1,0xafffaf); Figure=1; N1=100; k=0;a=0;b=20;
for(i=1;i<N1;i+=1) { x=i*4*PI/N1; y=cos(x)+b*sin(x)/(x*x); if(y>2) continue;
D[k+k]=x/PI; D[k+k+1]=y;k+=1;} SetPen(2,0xff); Polyline(k,D);
N1=1000; N=6; f=0; k=0; c=PI/N; n=0; z=cos(c); z1=2;
for(i=1;i<N1;i+=1) { x=i*4*PI/N1; y=cos(x)+b*sin(x)/(x*x);
if(z1>z) {if(y<=z) f=1;} else {if(y>=z) f=1;}
if(f>0) {D[k+k]=x/PI; D[k+k+1]=y;k+=1;n+=1;z1=z;z=cos((k+1)*c);f=0;}
}
SetPen(2,0xff0000); Plot("OVALFILL,0,@k,XY,3,3,",D);
//TextAt(100,10,"k=%d, n=%d",k,n);
}#v07=?>A
<Clet2020 Script>//[9] sun
```

```
int i,j,k,n,N,N1,f,Figure; double x,y,z,z1,a,b,c,d,D[400],S[400];
main(){ SetAxis(X_AXIS,0,0,10,"a.u.; ;5;10;");SetAxis(Y_AXIS,0,0,4,"#ifk#t;0;1;2;3;4;");
DrawFrame(FRAME_SCALE,1,0xafffaf); b=20;
N1=1000; N=6; f=0; k=0; c=PI/N; n=0; z=cos(c); z1=2;
for(i=1;i<N1;i+=1) { x=i*4*PI/N1; y=cos(x)+b*sin(x)/(x*x);
if(z1>z) {if(y<=z) f=1;} else {if(y>=z) f=1;}
if(f>0) {D[k+k]=x/PI; D[k+k+1]=y;k+=1;n+=1;z1=z;z=cos((k+1)*c);f=0;}
}
for(i=0;i<k;i+=1) {x=D[i+i]; S[0]=1;S[1]=x;S[2]=5;S[3]=x;
Draw("LINE,0,2,XY,0",S);}
TextHang(6,0.9,0,"Band1");TextHang(6,1.8,0,"Band2");
TextHang(6,2.5,0,"Band3");TextHang(6,3.5,0,"Band4");
}#v07=?>A
```

As observed in the solar system, N=6, planets (n=1 and n=2) have been burned off by the sun duo to solar extreme high temperatures, the inner planets (Mercury, Venus, Earth and Mars) belong to the first band, the outer planets (Jupiter, Saturn, Uranus and Neptune) belong to the second band (in terms of band theory, re-use index n=1,2,…N in the second band), while Ceres (dwarf) locates in a forbidden band. Ceres plays a role of impurity as if in semiconductor in electronics. This situation indicates that phase change ΔR reaches its maximum value near the Ceres's location. So, we estimate that the r_R should be a radius between Ceres and Jupiter.

Before Gauss, the famous mathematician Euler had developed a method for calculating the orbits of planets. However, this method is too cumbersome. Gauss is determined to find a simple and feasible method. On the basis of predecessors, Gauss created a new theory of computation of planetary orbits with his outstanding mathematical ability after hard calculation. Based on Piazzi's observation data, he used this method to calculate the orbit shape of Ceres in just one hour and indicate when it will appear in which sky. On the night of December 31, 1801, German astronomer Olbers aimed a telescope at this sky during the time predicted by Gauss. As expected, Ceres miraculously appeared again!

At the end of 2003 and the beginning of 2004, the Hubble Space Telescope took the appearance of Ceres for the first time, and found that it was quite spherical. It was believed that Ceres had complex terrain, and some astronomers even speculated that Ceres had an icy mantle and a metal core.

5. Period of sunspot cycle

The **coherence length** of waves is usually mentioned but the **coherence width** of waves is rarely discussed in quantum mechanics, simply because the latter is not a matter for electrons, nucleon, or photons, but it is a matter in astrophysics. The analysis of observation data tells us that on the planetary scale, the coherence width of relativistic matter waves can extend to 1000 kilometers or more, as illustrated in Fig.6(a), the overlap may even occur in the width direction, thereby bringing new aspects to wave interference.

In the solar convective zone, adjacent convective rings form a top-layer flow, a middle-layer gas, and a ground-layer flow. Considering one convective ring at the equator as shown in Fig.6(b), there is an apparent velocity difference between the top-layer flow and the middle-layer gas, where their relativistic matter waves are denoted respectively by

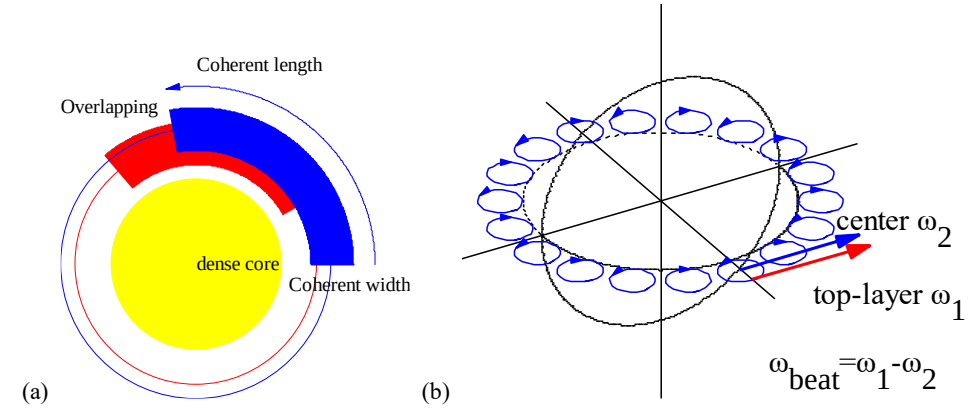

Fig.6 (a) Illustration of overlapping in the coherent width direction. (b) Convective rings at the equator.

$$\psi = \psi_{top} + C\psi_{middle}$$
$$\psi_{top} = \exp[\frac{i\beta}{c^3}\int_L (v_1 dl + \frac{-c^2}{\sqrt{1-v_1^{\,2}/c^2}}dt)]$$
$$\psi_{middle} = \exp[\frac{i\beta}{c^3}\int_L (v_2 dl + \frac{-c^2}{\sqrt{1-v_2^{\,2}/c^2}}dt)] \quad . \tag{15}$$

Their interference in the coherent width direction leads to a beat phenomenon

$$|\psi|^2 = |\psi_{top} + C\psi_{middle}|^2 = 1 + C^2 + 2C\cos[\frac{2\pi}{\lambda_{beat}}\int_L dl - \frac{2\pi}{T_{beat}}t]$$
$$\frac{2\pi}{T_{beat}} = \frac{\beta}{c^3}(\frac{c^2}{\sqrt{1-v_1^{\,2}/c^2}} - \frac{c^2}{\sqrt{1-v_2^{\,2}/c^2}}) \simeq \frac{\beta}{c^3}(\frac{v_1^{\,2}}{2} - \frac{v_2^{\,2}}{2}) \quad . \tag{16}$$
$$\frac{2\pi}{\lambda_{beat}} = \frac{\beta}{c^3}(v_1 - v_2); \quad V = \frac{\lambda_{beat}}{T_{beat}} = \frac{1}{2}(v_1 + v_2)$$

Their speeds are calculated as

$$v_1 \approx 6100\,(m/s) \quad (\approx \text{observed in Evershed flow})$$
$$v_2 = \omega r_{middle} = 2017\,(m/s) \quad (\text{solar rotation}); \quad . \tag{17}$$

Where, regarding Evershed flow as the eruption of the top-layer flow, about 6 (km/s) speed was reported [13]. Alternatively, the top-layer speed v_1 also can be calculated in terms of thermodynamics, to be v_1=6244 (m/s) [6]. Here using v_1=6100 (m/s), their beat period T_{beat} is calculated to be a value of 10.95 (years), in agreement with the sunspot cycle value (say, mean 11 years).

$$T_{beat} \simeq \frac{4\pi c^3}{\beta\left(v_1^{\,2} - v_2^{\,2}\right)} = 10.95\,(years) \quad . \tag{18}$$

```
<Clet2020 Script>// [9]
double beta,H,M,N,dP[20],D[2000],r,rs,rot,x,y,v1,v2,K1,K2,T1,T2,T,Lamda,V; int i,j,k,s;
int main(){beta=2.956391e10; H=SPEEDC*SPEEDC*SPEEDC/beta;
M=1.9891E30; rs=6.95e8;rot=2*PI/(25.05*24*3600);v1=rot*rs;K1=v1*v1/2;//T1=2*PI*H/K1;
v2=6100; K2=v2*v2/2;T2=2*PI*H/(K2-K1);T=T2/24*3600*365.2422;
Lamda=2*PI*H/(v2-v1);V=Lamda/T2;s=1;
SetViewAngle("temp0,theta60,phi-60");
DrawFrame(FRAME_LINE,1,0xafffaf);Overlook("2,1,60", D);
TextAt(10,10,"v1=%d, v2=%d, T=%.2f y, λ=%e, V=%d",v1,v2,T, Lamda,V);
SetPen(1,0x4f4fff); for(i=0;i<18;i+=1) {v1=i*2*PI/18; x=70*cos(v1);y=70*sin(v1);Ring();}
SetPen(2,0xff0000);Draw("ARROW,0,2,XYZ,15","80,0,0,80,60,0");
```

TextHang(100,20,0,"top-layer ω#sd1#t"); SetPen(2,0x0000ff);
Draw("ARROW,0,2,XYZ,15","70,0,0,70,60,0");
TextHang(50,60,0,"center ω#sd2#t");TextHang(140,-30,0," ω#sdbeat#t=ω#sd1#t-ω#sd2#t");
}
Ring(){ k=0;N=20; r=10;
for(j=0;j<N+2;j+=1) {k=j+j+j; v2=s*j*2*PI/N; D[k]=x+r*cos(v2);D[k+1]=y+r*sin(v2); D[k+2]=0;}
Plot("POLYLINE,4,22,XYZ,8",D)s*=-1;}
#v07=?>A

The relative error to the mean 11 years is 0.6% for the beat period calculation using the relativistic matter waves. This beat phenomenon turns out to be a **nucleon density oscillation** that undergoes to drive the sunspot cycle evolution. The beat wavelength λ_{beat} is too long to observe, only the beat period is easy to be observed.

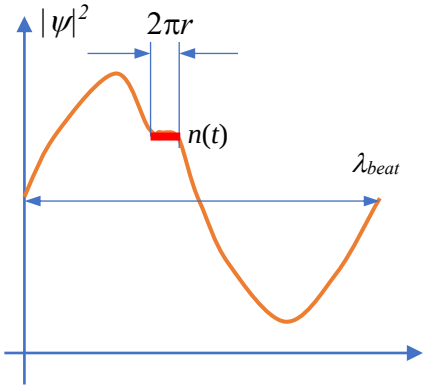

Fig.7 The equatorial circumference $2\pi r$ only occupies a little part of the beat wavelength, what we see is the expansion and contraction of the nucleon density.

As shown in Fig.7, on the solar surface, the equatorial circumference $2\pi r$ only occupies a little part of the beat wavelength, what we see is the expansion and contraction of the nucleon density.

$$\frac{2\pi r}{\lambda_{beat}} = 0.0031 \ . \tag{19}$$

This nucleon density oscillation is understood as a new type of nuclear reaction on an astronomic scale.

6. Conclusions

In recent years, de Broglie matter wave has been generalized to the solar system on planetary scale, this approach provides a new method for testing quantum gravity effects. This paper shows that the generalized matter wave can quantize the orbits of eight planets correctly, but the orbit of Ceres (dwarf) is forbidden in terms of the quantum gravity theory. This forbidden orbit successfully explains why Ceres is almost extinct in the solar system.

References

[1] de Broglie, L. (1923) Waves and Quanta. Nature, 112, 540. https://doi.org/10.1038/112540a0
[2] de Broglie, L. (1925) Recherches sur la théorie des Quanta, Translated in 2004 by A. F. Kracklauer as De Broglie, Louis, on the Theory of Quanta. https://doi.org/10.1051/anphys/192510030022
[3] Marletto, C. and Vedral, V. (2017) Gravitationally Induced Entanglement between Two Massive Particles Is Sufficient Evidence of Quantum Effects in Gravity. Physical Review Letters, 119, Article ID: 240402. https://doi.org/10.1103/PhysRevLett.119.240402
[4] Guerreiro, T. (2020) Quantum Effects in Gravity Waves. Classical and Quantum Gravity, 37, Article ID: 155001. https://doi.org/10.1088/1361-6382/ab9d5d
[5] Carlip, S., Chiou, D., Ni, W. and Woodard, R. (2015) Quantum Gravity: A Brief History of Ideas and Some Prospects, International Journal of Modern Physics D, 24, Article ID: 1530028. https://doi.org/10.1142/S0218271815300281
[6] Cui, H.Y. (2021) Relativistic Matter Wave and Quantum Computer. Kindle eBook, Amazon, Seattle.
[7] NASA. https://solarscience.msfc.nasa.gov/interior.shtml
[8] Schneider, S.E. and Arny, T.T. (2018) Pathways to Astronomy. 5th Edition, McGraw-Hill Education, London.
[9] Clet Lab (2022) Clet: C Compiler. https://drive.google.com/file/d/1OjKqANcgZ-9V56rgcoMtOu9w4rP49sgN/view?usp=sharing
[10] Orbital Debris Program Office, (2018) History of On-Orbit Satellite Fragmentations. 15th Edition, National Aeronautics and Space Administration, Washington DC.
[11] Wright, D. (2007) Space Debris. Physics Today, 10, 35-40. https://doi.org/10.1063/1.2800252
[12] Tang, Z.-M., Ding, Z.-H., Dai, L.-D., Wu, J. and Xu, Z.-W. (2017) The Statistics Analysis of Space Debris in Beam Parking Model in 78˚ North Latitude Regions. Space Debris Research, 17, 1-7.
[13] Cox, N. (2001) Allen's Astrophysical Quantities. 4th Edition, Springer-Verlag, Berlin. https://doi.org/10.1007/978-1-4612-1186-0
[14] wikipedia, https://en.wikipedia.org/wiki/List_of_longest-living_organisms#Animals
[15] Cui,H.Y. (2022) Study of Earthquakes in Japanese Islands Using Quantum Gravity Theory with Ultimate Acceleration, viXra:2209.0149, 2022. https://vixra.org/abs/2209.0149
[16] Cui,H.Y. (2023) Determination of Solar Radius and Earth's Radius by Relativistic Matter Wave, Journal of Applied Mathematics and Physics, 11, 1, DOI: 10.4236/jamp.2023.111006
[17] Cui,H.Y. (2023) Biological Clock of Relativistic Matter Wave and Calculation of Human Mean Lifespan 84 Years. Modern Physics, 2023, 13(2): 28-41. DOI: 10.12677/mp.2023.132005